STRONG SCATTERERS AND 1-D BORN INVERSION

L. J. Bond and H. Zhang

NDE Centre, Department of Mechanical Engineering
University College London
London, WCI E 7JE, United Kingdom

James H. Rose

Ames Laboratory, USDOE
Iowa State University
Ames, IA 50011, U.S.A.

INTRODUCTION

Ultrasonic flaw sizing is critical in nondestructive evaluation. However, the data available for sizing are often quite limited. For example, it is common to have a single pulse-echo (back scattered) wavetrain of limited bandwidth: i.e. it contains wavelengths that are comparable to and larger than the dimensions of the flaw. On the other hand a fair amount is often known about the nature of the expected range of flaws. It may be known that the flaw is a void, or a crack or an inclusion of a certain material type. In addition the expected shape for a flaw may be known (e.g. the flaw may be known to be a spherical flaw of unknown radius). The problem is then to determine the relevant unknown features of the flaw from the available data.

In essence the information content of a single pulse-echo signal can be divided into amplitude data and timing data. The use of amplitude data in sizing is based on the common-sense observation that, other things being equal, larger flaws will reflect more ultrasound. Similarly timing data is closely related to the length of time it takes the incident pulse to traverse the flaw. Two types of timing data have been used. First the flaw's size can be estimated from the total duration of the reflected pulse. Second adequate low frequency data makes it possible to estimate the point in time in the echo signal that corresponds to scattering from the flaws centroid. Consequently it is possible to estimate the time between the reflection from the flaw's front surface and from the centroid. This leads to an estimate for the flaw's radius.

Each piece of information mentioned above has served as the basis for a flaw sizing algorithm. For example, the commercially used dB drop method [1] is based on the amplitude of the signal. Similarly the total duration of the signal is used to estimate the flaw size in the satellite pulse method [2]. There the duration is measured as the time between the front surface reflection and a suitable trailing wave (the "satellite" pulse). Finally, the one dimensional inverse Born approximation (1-D IBA) estimates the radius from the determination of the difference in timing between the front-surface echo and the centroid. The present paper is a progress report on an attempt to combine the use of 1-D Born approximation and aspects of the satellite-pulse method for sizing flaws. Our approach is numerical and focuses on spherical voids (radii 50 to 1000 μm) in Titanium.

It is hoped that, once this relatively simple problem is understood, the analysis can be extended to allow flaw sizing in more complicated circumstances. Last year we reported similar results for the case of weakly scattering flaws [3]; in contrast to voids (strong scatterers) which are considered here.

The 1-D IBA requires an estimate for the zero-of-time (ZOT). Different choices for the ZOT result in different estimates for the flaw's radius. As discussed by Bond et al. [3], a plot of the inverse Born estimate for the flaw's radius as a function of the ZOT, provides a characteristic signature; this plot has been christened the Born Radius/Zero-of-Time Shift Domain (BR/ZOTSD) signature. It contains both types of timing information mentioned above. First the distance between two characteristic nulls (discussed extensively below) yields the same information as the satellite pulse method. Secondly, the radius estimate at the correct ZOT is the desired output of the Inverse Born Approximation.

Consideration of both kinds of timing information in the BR/ZOTSD signature should, in principle, leads to a more accurate radius estimate than using either type of information alone. Below we focus on the characteristic null's in the BR/ZOTSD signature and show that they result from the same features in the flaw's time domain response as are used in the satellite pulse method.

SCATTERING BY SPHERICAL VOIDS

Elastic wave scattering from spherical voids in an isotropic and otherwise homogeneous material is accurately described in the low and intermediate frequency regime by the theory of Ying and Truell [4]. However, the mathematical form of this theory (a tensor partial wave expansion) does not provide, in any direct way, a physical interpretation of the scattering process. In particular it is difficult to put Ying and Truell theory on a common footing with the various physically motivated approximate methods such as elastodynamic ray theory.

An alternative model for scattering has been proposed by Zhang and Bond [5]. This is a combination of ray theory, for the front surface reflection, with a partial wave expansion approach for both the spreading part of the direct reflection and the creeping wave components. This model is more easily related to the physical scattering process. The far field impulse response function given for a void in Titanium [5] is shown as Figure 1. An alternative model, based on MOOT has been provided by Opsal and Visscher [6] and this gives results which are almost identical to those shown as Figure 1.

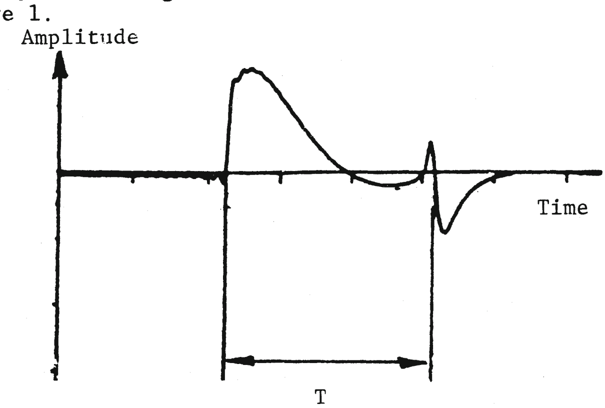

Fig. 1. Time domain response for a spherical void in Titanium [5]. The downgoing arrow represents the delta-function response due to the incident delta-function plane wave. The second return, marked with the vertical bar, is due to the surface skimming longitudinal (creeping) waves.

A key to understanding the time domain signature, and also the corresponding BR/ZOTSD signatures, is the prediction of the arrival time for the second arrival, the creeping wave component or satellite pulse seen in Fig.1. It has been reported [7] that the separation of the pulses (see Fig. 1) can be predicted by the relationship;

$$T = (1/c + \pi/2v)d \tag{1}$$

where c is the longitudinal wave velocity, v is the creeping wave velocity and d is the void diameter.

The creeping wave velocity to be used in calculations with Eq. 1 is not however obvious as various publications give values for creeping wave velocities that cover the range 0.8c to 0.95c. Gruber et al. [7] give an experimental value for the creeping wave velocity in Titanium of 0.87c which we adopt below.

The scattering models, mentioned above, have been used in this paper to estimate the radii of spherical voids using the Inverse Born Approximation. In particular they have been used to test the utility of flaw sizing in the BR/ZOTSD.

1-D BORN INVERSION

Various reviews of 1-D Born Inversion have been published elsewhere, so only the very briefest outline is given here [3,8,9]. The Born algorithm is applied to the impulse response function after the choice of the zero-of-time (ZOT). For a weakly scattering spherical flaw the approximate ZOT is indicated by the midpoint between the front and back-surface delta-function reflections (see Ref. 3). For such a response function the IBA algorithm estimates an ideal step shaped characteristic function for the correct ZOT. However for real flaws such as voids, measured using systems with a bandwidth limitation, the time domain signatures, impulse responses and characteristic functions are all more complicated than those for simple weak scatterers; hence the problems associated with ZOT selection.

The "correct" zero-of-time is conventionally sought after a nominal ZOT has been selected on the basis of the time domain signature, by a series of iterations which look at features in the characteristic function; and small shifts in the value selected for the ZOT are made. For each time shift the Born radius varies as it is evaluated by two techniques which are known as (i) the 50% contour and (ii) the area/peak for the characteristic function. Both methods for estimating the radius can be used to generate a BR/ZOTSD signature. Below we focus primarily on signatures generated by using the area/peak method of estimating the radius.

BORN RADIUS/ZERO-OF-TIME SHIFT DOMAIN; STRONG SCATTERERS

An example of a BR/ZOTSD signature evaluated using the Born radius given by the area/peak technique for a 200 μm radius void (using simulated data) is shown in Fig. 2. Such signatures have been reported in earlier studies but they were not then used to size flaws [7,10]. The bandwidth employed for the data used to give Fig. 2 has traditionally been considered to be "wide-band", however the signature does not take the form of a simple inverted parabola which was found for wide band weak scattering data. To investigate the variation in this BR/ZOTSD signature, with bandwidth, data for the case of 0 to 100 MHz (0-30 ka: k is the wave number and a the flaw radius) was evaluated. The resulting BR/ZOTSD signature is shown as Fig. 2. The third curve shown in Fig. 2 is the BR/ZOTSD signature obtained for the 50% contour data; it is seen to give the correct radius estimate at the true ZOT.

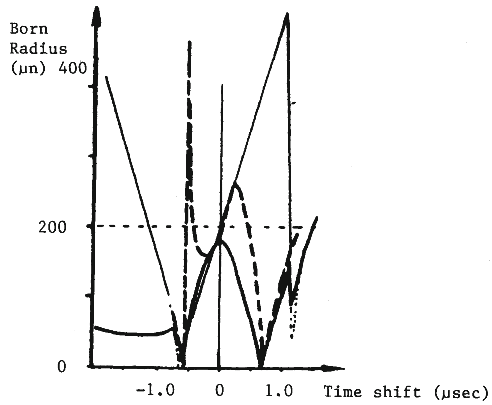

Fig. 2. BR/ZOTSD signatures for various bandwidth data for a 200 μm void in Titanium. (i)--0.5-15 MHz (0.1-3 ka); (ii) --0-100 MHz, and (iii) -- 50% contour variation for 0-100 MHz data.

Features in the BR/ZOTSD signature can be related to several factors including; i.ka range. ii. Flaw radius to center frequency ratio and iii. Matrix material properties. A series of investigations were performed to seek to understand the signature and its possible use to size voids. This study is reported below, with additional results elsewhere [11].

When the signatures obtained for the void (Fig. 2) are compared with those obtained for a weak scatterer [3] there are both similarities and contrasts. Both signatures vary as a function of bandwidth and with wide-band data take a form close to an inverted parabola, which is similar to the corresponding scatterers area function. For both strong and weak scatterers there are two "Null" points. The nulls correspond to the front surface echo and the satellite pulse shown in the impulse response function (Fig. 1). For the case of a 200 μm radius void using wide-band data (Fig. 2) one finds that the separation of the nulls in the BR/ZOTSD signature is very close to that required for the longitudinal wave to travel a distance of "4d".

It was reported earlier [3] that the null separation of "apparent transit time" in the BR/ZOTSD domain signature for a weak scatterer is related to the zero crossings in the impulse response function by the factor 3/4. When the time domain signature for the void is considered (Fig. 1), it was proposed that Eq. (1) can be used to predict the separation of the zero crossings. It is then found that if Eq. (1) is considered for the void it can be used with the same scale factor of 3/4 in an ad hoc way to relate the time domain pulse separation and BR/ZOTSD null separation. The scale factor of 3/4 comes from the two integrations which are used to convert the impulse response data in the time domain to the BR/ZOTSD signature, using the area/peak technique for radius estimation [12]. The resulting relationship is proposed for the null separation for voids in the BR/ZOTSD signature;

$$T = 3/4(1/c + \pi/2v)d \qquad (2)$$

where, for Titanium, c=6130 m/sec and v=0.87c for a range of voids [7,5].

Results for a series of voids in Titanium obtained through the use of the Born Inversion Algorithm for a range of bandwidths are shown in Fig. 3, together with the data obtained with Eq. 2. The ideal data, from Eq. 2, and two cases of assumed wideband data are shown in Fig. 3a. Two cases if limited bandwidth data are shown in Fig. 3b. These are the case of data

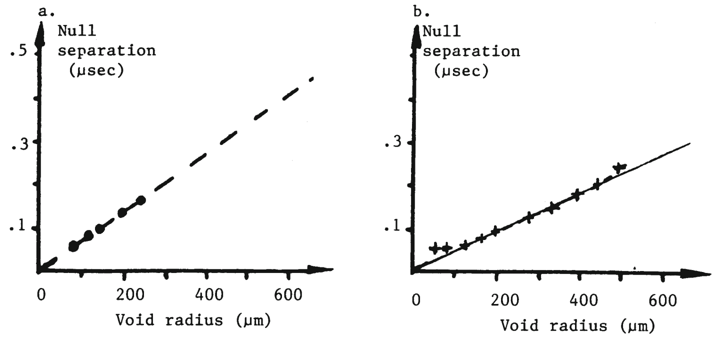

Fig. 3. Flaw Radius estimated from "null separation" for voids in Titanium; a. -- using Eq. 2; • IBA with fixed 0.5 to 40 MHz; b. -- IBA with 0.5 to 2.5 ka data; + IBA with fixed 2-12 MHz bandwidth.

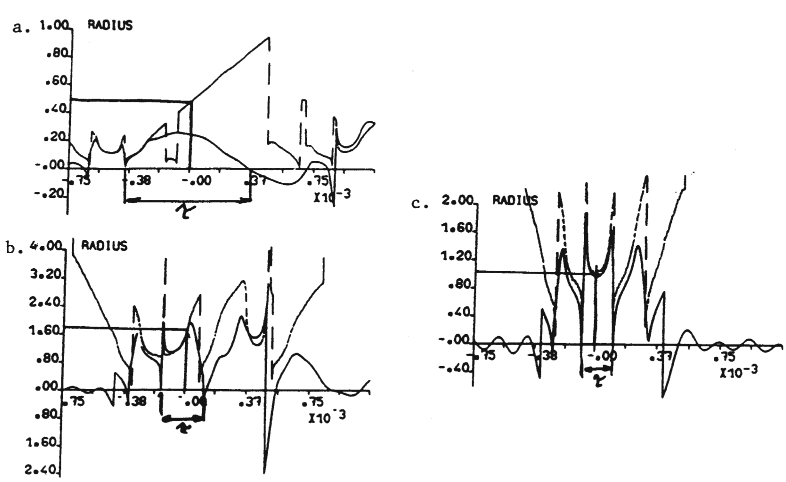

Fig. 4. BR/ZOTSD signatures for spherical voids in Titanium for 2-12 MHz fixed bandwidth incident longitudinal waves. a. 500 μm radius. b. 200 μm radius and c.

for a fixed 0.5 to 2.5 ka bandwidth at each point and for a fixed 2 to 12 MHz bandwidth, for which the void radius was varied, to simulate a 100 μm radius. τ is null separation. 50% at ZOT is shown. In all cases the line is BR from the 50% contour data real experimental situation. Examples of the BR/ZOTSD signatures from the 2-12 MHz fixed bandwidth series are shown as Fig. 4. It can be seen in Fig. 3 that the radius is accurately estimated using the BR/ZOTSD signature and Eq. 2.

It is found that the form of the signature, shown as Fig. 4, can be used as a good guide to the transducer/defect (ka) and bandwidth match which has been employed in a particular measurement. The case of a poor bandwidth match can thus be identified and measurement repeated with a better transducer bandwidth/defect size match. In almost all cases the 50% contour at the true ZOT continues to give a good estimate for the defect radius. The selection of the central point between the nulls is a good guide for the location of the true ZOT. When material data is available a correction factor for the loss of symmetry can be employed. For bandlimited data additional factors such as the window function which is employed need consideration. In almost all cases a suitable calibration curve can be generated.

MATERIAL PROPERTY VARIATION AND THE VOID BR/ZOTSD SIGNATURE

The BR/ZOTSD signature for spherical voids in a variety of isotropic and otherwise homogeneous elastic solids are presented below. In each case the void was assumed to have a 200 μm radius and the bandwidth of the ultrasonic system was assumed to range from 0.5 to 40 MHz. The host materials were characterized by a constant density, e=4.5 gm/cm, and a constant longitudinal velocity, c=6130 m/sec, and a varying velocity ratio, η=shear-velocity/longitudinal-velocity. The resulting BR/ZOTSD signatures are shown in Fig. 5 for 0.4 < η < 0.6.

The structure of the BR/ZOTSD signatures shown in Fig. 5 can be described as follows. Each shows an initial null that occurs at t=-3d/4c. This value of t is independent of the velocity ratio. The second null occurs at a time somewhat greater than t=+3d/4c. The value of t for this null depends on the velocity ratio; it becomes larger as η decreases. Presumably the shift in the second null depends on variations in the creeping wave velocity, which decreases as η decreases. The dependance of the time of occurance of the second null can be seen in Fig. 6. Here the time between nulls, τ; for the BR/ZOTSD are plotted as a function of η and i. η = 0.6 -- ii. η = 0.5 -- iii. η = 0.45 -- and iv. η = 0.4 compared with the time duration between zeros in the impulse response function (Fig. 1). We note that τ for the BR/ZOTSD is nearly equal to 3/4 that for the impulse response function. There is however some residual dependance on η (less than + 15% for almost all engineering materials). This dependance is the subject of ongoing study [5]. Finally we note that the IBA (using the 50% contour to estimate radius) gives the radius correctly (200 + 2 μm) for 0.4 < η < 0.6 if the correct ZOT is known.

CONCLUSIONS

It has been shown that the nulls in the BR/ZOTSD signature given through the use of the IBA technique measures the same features in the flaw's scattered wave field as are used in the satellite pulse technique. This approach was tested using synthetic data for spherical voids in Titanium and good estimates for the size of the flaws were obtained.

The following points were emphasized. First a new model (based on the fundamental physics) was used to model the impulse response function (flaw signal). Second the BR/ZOTSD was shown to depend in a simple way on transducer bandwidth. Hence it should be possible to use calibration curves to correct for this effect. Third the results showed that the BR/ZOTSD signature can be used to estimate defect/transducer ka

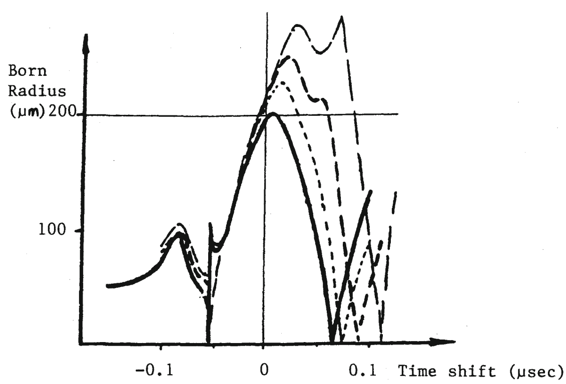

Fig. 5. BR/ZOTSD signatures for 200 m radius voids, 0.5 to 40 MHz data, fixed longitudinal wave velocity and with variation in η = Vs/Vc.

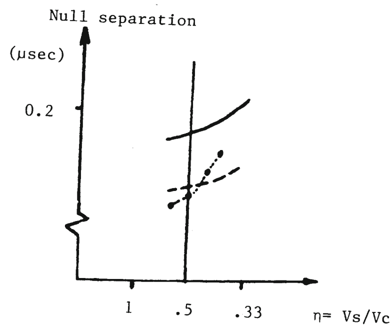

Fig. 6. Variation of Null separation in i. -- time domain, ii. -- with factor of 3/4 applied to time domain, and iii. • • • the BR/ZOTSD; for range of media, with Vc fixed at 6130 m/sec and Vs varied.

and bandwidth match as well as an estimate for the correct ZOT. Finally it was shown how the diameter of spherical voids can be determined from measurements in the BR/ZOTSD WITHOUT the need to explicitly estimate the correct zero-of-time.

ACKNOWLEDGMENT

Part of this work was supported by the Director of Energy Research, Office of Basic Energy Sciences, U.S.A. and performed while Dr. Bond was a Visiting Scientist at the Ames Laboratory, Ames, Iowa, which is operated for the U.S. Department of Energy by Iowa State University under Contract No. W-7405-ENG-82.

The UK part of the work was completed while Dr. H. Zhang (Institute of Acoustics, Academia Sinica, Beijing, China) was a British Council funded visiting scientist at University College London, UK.

REFERENCES

1. Gilardoni Handbook (1981) Nondestructive Testing, Gilardoni S.p.A. (Como, Italy).
2. Gruber, G. J. (1980), Defect identification and sizing by the ultrasonic satellite pulse method, Journal of NDE, 1, p. 263.
3. Bond, L. J., Chaloner, C. Wormley, S. J., Neal, S. P., and Rose, J. H. (1987), Recent advances in Born Inversion (weak scatterers), in Review of Progress in QNDE, Vol. 7, Ed. D. O. Thompson and D. E. Chimenti, Plenum (New York), p. 437-444.
4. Ying, C. C. and Truell, R. (1956), Scattering of a plane longitudinal wave by a spherical obstacle in an isotropic elastic solid, J. Appl. Phys. (1956), Vol. 27, p. 1086-1097.
5. Zhang, H. and Bond, L. J. (1988), Ultrasonic scattering by spherical voids ULTRASONICS (in preparation).
6. Opsal, J. L. and Visscher, W. M. (1985), Theory of elastic wave scattering: application of methods of optimal truncation, J. Appl. Phys. Vol. 58, p. 1102-1115.
7. Gruber, G. J., Hendrix, G. J. and Hueller, T. A. (1985), Exploratory development for high reliability flaw characterization module. Technical report AFWAL-TR-84-4172, US Air Force Wright Aeronautical Laboratory.
8. Chaloner, C and Bond, L. J. (1987), Investigation of the 1-D inverse Born Technique, IEE Proceedings, Vol. 134, Pt. A., p. 257-265.
9. Rose, J. H. and Krumhansl, J. A. (1979), Determination of flaw characteristics from ultrasonic scattering data, J. Appl. Phys. Vol. 50, p. 2951.